Arabian Journal of Geosciences (2020) 13: 687
https://doi.org/10.1007/s12517-020-05664-5

ORIGINAL PAPER

Mapping and monitoring land use and land cover changes in Mellegue watershed using remote sensing and GIS

Okba Weslati[1] · Samir Bouaziz[1] · Mohamed Moncef Serbaji[1]

Received: 25 November 2018 / Accepted: 1 July 2020 / Published online: 17 July 2020

Abstract

The supervised classification maximum likelihood was applied in this study. It aimed to visualize the land use/land cover changes in the Mellegue catchment, using multispectral satellite data of Landsat imagery for a specific study period from 2002 to 2018. This classification was built based on ground truth data collected for nine classes. These data were entered subsequently in the ENVI software to operate the classification process. Then, the results were refined using the GIS tool, by ArcGIS software, which required a visual interpretation and expert knowledge of the area. According to the cross-tabulation matrix and classification results, it was found that major changes have occurred during the study period causing serious degradation of the environment and ecosystem.

Keywords Maximum likelihood · Supervised classification · Land use/land cover · Mellegue · GIS

Introduction

Land use/land cover (LULC) change occurs within the watershed can affect not only the environment, ecosystem, climate and hydrology but also the water balance and water resources. Evidently, this interaction is responsible for the fluctuation of the water balance components as their magnitude, including the increase in downstream flooding and the decrease in the long-term groundwater supplies (Bronstert et al. 2002; Kumar et al. 2017).

Besides affecting the water supply quantity, land use change (especially urbanization) is also responsible for deteriorating the water quality within the watershed by changing the composition of surface water and increasing the susceptibility of nutriments. In addition, the water transport issue can result in irretrievable phenomena such as desertification, water salinization, erosion and the reduction of annual production of yields (Lubowski et al. 2006). On the other hand, abundant agricultural lands are directly linked to the application of chemical products like fertilizers and manure which act severely in poisoning the water system (Johnes and Heathwaite 1997). Yet, some other specific lands are subject to evapotranspiration fluctuation which can severely disturb the hydrologic cycle and, consequently, unbalance the annual water resources (Fohrer et al. 2001). This was linked to the alteration of surface temperature, stormwater runoff, carbon sequestration and biodiversity (Pauleit et al. 2005).

To have an in-depth analysis of the fast land use changes, it is compulsory to have a substantial amount of data about the earth's surface. As a matter of fact, Taylor (2002) has quantified the land use demand according to a specific equilibrium between the production and consumption of resources. Unfortunately, the conversion of land use has been randomly and unreasonably applied without any restrictive laws, which may severely deteriorate the ecosystem and the environment. This has made planners, policy makers and resource managers rely on LULC change detection as an efficient mechanism in detecting major anomalies like reservoir sedimentation and remarkable changes in streamflow patterns. These impacts may damage economies and ruin water projects generally dedicated for long-term sustainability (Biswas 1990; Bronstert et al. 2002).

Responsible Editor: Biswajeet Pradhan

✉ Okba Weslati
okba.weslati@gmail.com

Samir Bouaziz
samir.bouaziz@enis.rnu.tn

Mohamed Moncef Serbaji
mohamed-moncef.serbaji@enis.tn

[1] Laboratory of Water, Energy, Environment, National Engineering School of Sfax, Road of Sokra 3 km, 3038 Sfax, Tunisia

Remote sensing (RS) and GIS have served for many years in mapping and assessing LULC change by providing worthy quantitative and timely information (Michalowska et al. 2016). With the advance of technology, RS and GIS have become vital tools in studying abnormal phenomena related to LULC changes. In fact, Baynard (2013) has pointed to the importance of RS in analysing the human-environment interaction and studying the physiological behaviour of vegetation and forests. He used satellite imagery to identify coal seam fire burning. Furthermore, he estimated the probabilities of such an event revealing the potential impacts on the environment and the ecosystem. Additionally, RS has contributed to analysing the physical parameters of ocean water (temperature, pressure, salinity, surface wind, emission of CO_2 and fuels). Multiple sensors and satellite images were also employed to quantify chlorophyll concentration and reveal its interaction with fauna resources. It serves for the study of the behaviour and the reproduction of certain fish species indicating their effects on the socio-economy of local areas (Treitz and Rogan 2004). It is also known that RS is a powerful tool in assessing the urbanization spread and population growth density. Therefore, the extension of urban areas is important to evaluate its effects on changing the neighbouring LULC classes (Dewan and Yamaguchi 2009). Moreover, RS intervenes in detecting archaeological sites (delimitation) and karst caves of prehistoric remains. It also helps in restoring previous architectural sites and reconstituting their networks. This leads us to conclude that the RS contributes significantly to the reconstitution of historical human ages.

The validity of RS always depends on field observation. Together, RS and field check build an efficient model for change detection and LULC classification. Despite the numerous preliminary procedures that need to be achieved (atmosphere calibration and gap fill) in order to compensate for the low-quality resolution and atmosphere influence, the importance of satellite images in LULC mapping and monitoring should not be underestimated. To get the most accurate results, some researchers suggest that LULC classification should be operated based on seasonal imagery in order to reduce the fluctuation of vegetation phenology from one season to another (Yacouba et al. 2009; Rimal 2011).

Change detection is usually operated based on multispectral satellite imagery, which caused a surge in the development of many classification algorithms over the previous years. Among these algorithms, the most popular are: Unsupervised classification, supervised classification, principal component analysis (PCA), vegetation index differencing, univariate image differencing, image regression and image rationing (Singh 1989). According to Berberoglu and Akin (2009), it seems that four change detection algorithms have been found to be efficient in the Eastern Mediterranean. These are the image differencing (agriculture land and forest assessment), the image rationing (correction of topology effects), the image regression (correct divergence from atmospheric condition and sun angle) and finally the change vector analysis (CVA) (radiometric calibration).

In this study, the supervised classification was operated using the maximum likelihood classifier. Post-classification was applied as a refinement to reduce classification errors and monitor land use changes through cross-tabulation.

The LULC changes assessment requires an effective and accurate operation with a readily available input data to identify all relative impacts associated to the watershed. Besides, the required preventive actions to reduce the negative impacts of land use changes are expensive and economically unbearable. Therefore, assessing the impact of land use change on the hydrological cycle via RS is considered a free and easy alternative which will help optimize watershed management and prevent natural crises (Telkar 2017).

This study, then, aimed to map and understand the LULC changes that occur in the watershed of Mellegue between 2002 and 2018. LULC change maps were built relying on Landsat Satellite data imagery using ENVI software. Field trips were required, at the initial steps, to get area samples for every LULC class and ultimately for post-classification refinement to validate the accuracy of the classification process. The shifts of land use, mainly those related to the conversion of forests and agricultural land into urban centres, between 2002 and 2018 were analysed statically in a change detection matrix. The resulting LULC changes through mapping and monitoring led us to deduce the potential impacts they have had on the Mellegue watershed.

Study area

The study area is located between 36° 25′ 50.43″, 35° 12′ 20.74″ north and 7° 11′ 30.98″, 8° 55′ 7.99″ east (Fig. 1). Being shared with Algeria, the Mellegue watershed covers an area of 10,500 km^2 while its perimeter is about 1053.8 km. Sixty percent of the catchment surface (6255.2 km^2) is located in Algeria but the outlet as well as the remaining area is situated in Tunisia.

It starts in the Mounts of TEBESSA, flows through the massif of AURES (Algeria) up to the southern end where it follows the long mountains range of Tunisian Atlas which separates the North from the Midland of Tunisia. The so-called Oued Mellegue is the main river of the catchment. It is considered, along with Sarrat River, as the largest rivers in the Northwest of the basin. It is 282 km long. It originates in Algeria, in the high plains along the northern hillsides of Nementcha massif near the village of Kenchela (Algeria) following the Southwestern-Northeastern direction of the Algerian-Tunisian Atlas until it ends in Jendouba (Tunisia) to join Oued Mejerda at the height 140 m above sea level (J.A.RODIER et al. 1981).

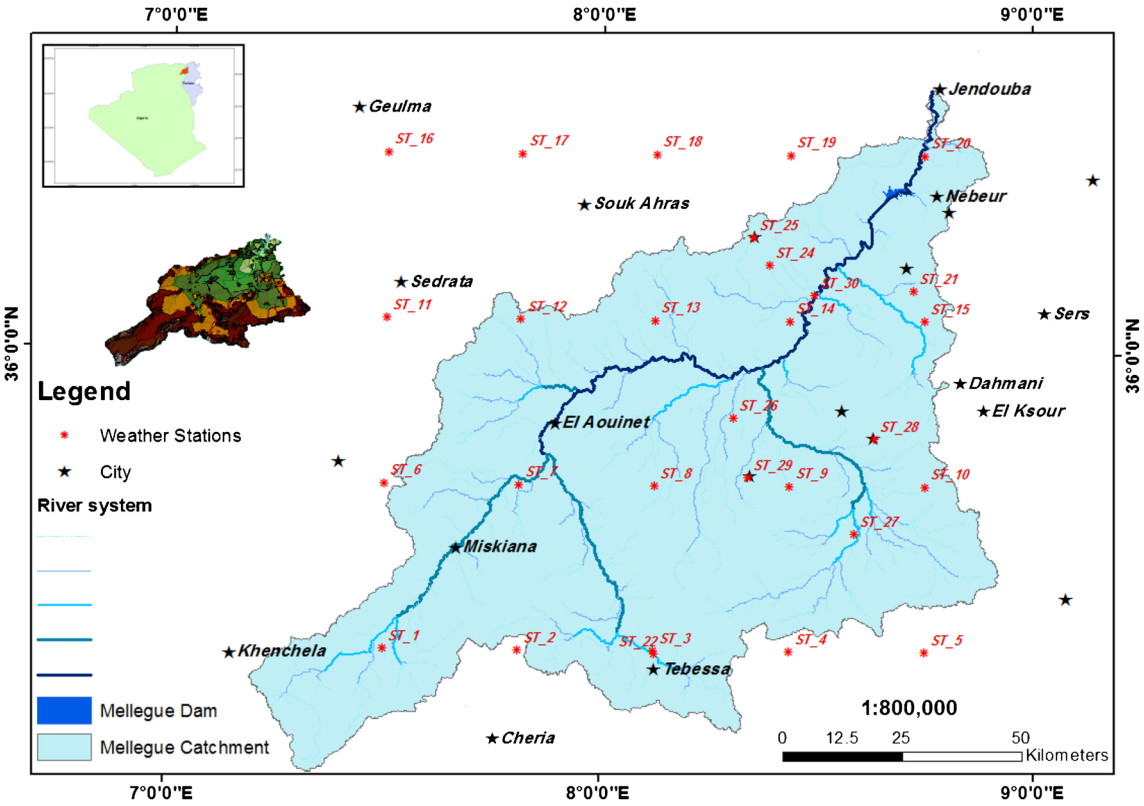

Fig. 1 Location of the study Area

Morphologically, the basin holds a moderate to strong relief where the slope varies from 0 to 25%. Geologically, the basin is mainly formed of limestone, marl, silts, alluvia and clay. It is also known for the manifestation of salt extrusions due to the faults' action that extrudes the Triassic evaporite and siliclastics. The study area is predominately covered with sedimentary rocks which illustrate a variety of formations of different ages (Mlayah et al. 2009, 2013, 2017; Belloula and Dridi 2015).

The basin contains a low variety of vegetation due to the semi-arid climate with a slight change to sub-arid in the north. Therefore, the climate is characterized by hot-dry summer and cold winter which is responsible for 50% of the annual rainfall. Hence, the average temperature is estimated at 17 °C annually with a slight variation of 1 to 2 °C. Such climate is known as a vulnerable ecosystem and so the impacts can be very intense. For this reason, land use change detection is essential for preserving the environment and land use management (Ahmadizadeh et al. 2014).

Materials and data collection

The main data used in this research are satellite files that contain the enhanced thematic mapper plus (ETM+) and operational land imager (OLI) accordingly to Landsat 7 and 8 for 2002 and 2018, respectively. The ETM+ and OLI are multispectral files that provide high-resolution image information of the Earth's surface. The image size is 185 × 170 km at a spatial resolution of 30 m except for thermal and panchromatic bands.

Other than the ETM+ and OLI, some ancillary data were used including areal imagery, digital elevation model (DEM), geological and topographical maps. Another essential step consisted in assembling ground truth data. In fact, this technique has great effects because the input file must be set before establishing the best classification. Furthermore, the supervised maps depend mostly on the accuracy of the ground truth data. The area of interest (AOI) is a ground truth sample set for each category. It means that the classification process uses the spectral signature of the AOI for each category to classify the images. The more AOIs are collected, the more accurate the map will be. In our study, the AOIs were collected via the global positioning system (GPS).

Image processing

Image processing is essential for enhancing classification accuracy. Uncertainties mixed up with error propagation in the image processing chain may lead to misclassification and false interpretation (Araya and Cabral 2010). Image processing has been applied successfully in our study via the ENVI software. Table 1 provides a series of processing procedures applied to

Table 1 Radiometric Correction in ENVI

Step	Process	Comments
I	Input Bands Images	Satellite data were downloaded from Earth Explore (https://earthexplorer.usgs.gov/). It contains ETM+ (for September 2002) and OLI (for January 2018). The study area requires two satellite images each (2002 and 2018) to cover it all.
II	Layer stacking	The layer stacking was built from the multiband georeferenced data. Four-layer stack files were processed which combined different band groups that form Landsat 7 and 8.
III	Edit Layer Stacking attributes (Band names and wavelength)	Editing layer stack attributes are essential, especially for the wavelength step. Modifying band names is helpful for the user to distinguish between the bands. But attributing the wavelength must be set according to Landsat 7 and 8 sensors.
IV	Mosaicking	Mosaicking of both 2002 and 2018 satellite images must be performed to cover the entire study area.
V	Clip mosaic file	This step consists of clipping the mosaic to the study area only. The income from eliminating the outside parts is found in optimizing the processing period.
VI	Radiometric Calibration	Radiometric correction (either Absolute and Relative) is so important in this case because the study involves comparing data sets over a period of time (from 2002 to 2018).
VII	Dark subtraction	Dark objects subtraction is an essential step, especially for multispectral data. It generally minimizes atmosphere scattering. This operation is based on the assumption that dark objects have no reflectance.
VII	Atmospheric Correction	Quick atmospheric correction (QUAC) is performed to eliminate to compensate the influence of the atmosphere. QUAC and Fast Line-of-sight Atmospheric Analysis of Spectral Hypercubes (FLAASH) represent the main two atmospheric correction models in ENVI. QUAC is very efficient with the multispectral radiance images. This is why it was selected.

Landsat Images in order to effectively assess the LULC changes.

Image classification

Satellite image classification is widely used in the study of spatial and temporal changes of land use for any chosen study area. The developed information produced from image classification is commonly applied to the LULC map. This resulting map is fundamental for evaluating ecosystem conditions and environmental trends. In this case study, the supervised classification was applied using the maximum likelihood which is a parametric classifier that uses a model based on the second-order statistic of the Gaussian probability density (Sundara Kumar et al. 2015).

The study area was classified based on the taxonomy of previous land use maps. The nomenclature includes nine main classes: built-up area, bare ground, lake, olive, arboriculture, viticulture, field crops, vegetable crops and forest (Table 2). The training samples were meticulously selected and refined in order to get a perfect classification. Some training samples were chosen according to ancillary data. Other AOIs were assembled during field trips using a GPS device. The mission was divided into two main stages. The first field visit was undertaken to collect and arrange AOIs for our supervised classification. Later assignment was considered as field check mission by visiting some patterns of classifying maps to ensure the validity and accuracy of the supervised classification. The AOI classes range from 3 to 144 polygons and total pixel size between 2049 and 12,485 pixels.

The separability of the training sites was achieved before launching the classification process. This action aimed to select the ideal samples in order to avoid confusion in interpretation during the classification step. Therefore, the AOIs separability was checked by the spectral separability test with reference to Jeffery–Matusita statistical Transformed divergence (Table 3). The resulting values from this divergence fluctuate between 0 and 2 where values close to 2 define a good separability but AOI pairs with values less than 1 were either rejected or combined into one class.

The accuracy assessment must be carried out for the interpretation of the supervised classification process. Each supervised classification cannot be considered as completed until its accuracy assessment is applied (Gómez and Montero 2011). The most known accuracy assessments work with an error matrix; it is powerful and effective in the change detection analysis. In addition to the overall accuracy, Kappa index was applied in this study by validating and assessing the image classification accuracy (Cohen 1960). Its application remains a subject of debate, though. Some authors doubt the Kappa efficiency especially in overestimating the agreement opportunities and underestimating the classification accuracy (Ma and Redmond 1995). Furthermore, there is always a confusion between similarity in

Table 2 Description of land use classes in the study area

Class	Description
Viticulture	It is the plantation of grapevines consumed as winemaking, raisins, table grapes and non-alcoholic grape juice.
Bare area	It refers to the unused lands, barren from any artificial cover and human interaction. They include bare rocks areas, sands and deserts. Food and Agriculture Organization (FAO) classify areas with less than 4% vegetative cover as bare land.
Built-up area	It describes lands with artificial cover due to human activities. They include human constructions (cities, towns, and transportations), extraction activities (open mines and quarries) or even waste disposal.
Lakes	They refer to areas that are naturally (lakes, rivers and snow) or artificially (canals, reservoirs, etc.) covered with water.
Olive	It is a Mediterranean evergreen tree or shrub. It is a short square tree with 8 to 15 m height and it is an important source of food and oil.
Vegetable crops	They refer to plants, usually herbaceous that are consumed by humans except for fruits, nuts, and cereal grains. They do include a certain class of fruits like tomatoes, courgettes and seeds such as pulses.
Arboriculture	This class consists of a variety of trees like shrubs, individual trees, perennial woody plants and fruit trees.
Field crops	It refers to any kind of crop that is grown for agricultural purposes. They are usually cultivated in large areas and they have an annual life cycle from 3 up to 5 months (grains, sugar, hay, cotton).
Forest	It is a large tract or area covered by trees, underbrush and woodland. They play a vital role as they intervene in environmental protection and life sustainability.

quantification and similarity of locations (Macleod and Congalton 1998).

All the above-cited actions were performed in this study to ensure the supervised classification accuracy. Despite each of the suggested actions has its weaknesses and deficiencies when applied separately, when integrated together, they can allow a reliable interpretation and enhance the classified maps.

NDVI

The NDVI is very popular and widely applicable in diverse fields, especially in remote sensing. The process runs based on chlorophyll absorption sensitivity. Although the NDVI is approved of by researchers, it is still vulnerable to large errors generated either from calculation or canopy background conditions (Becker and Choudhury 1988). In general, the NDVI equation is based on the reflectance curve of vegetation as defined by Van De Griend and Owe (1993) in the following equations:

Table 3 Separability of training samples from 2018 Landsat Image

Class	Jeffries-Matusita	Transformed divergence
Arboriculture	1.67	1.86
Vegetable crops	1.58	1.74
Forest	1.93	1.99
Field crops	1.67	1.82
Lake	1.98	2.00
Olive	1.58	1.81
Bare ground	1.64	1.82
Viticulture	1.69	1.95
Built-up area	1.86	1.90

$$NDVI = \frac{\mathrm{NIR}-\mathrm{RED}}{\mathrm{NIR}+\mathrm{RED}} \tag{1}$$

$$NDVI = \frac{\frac{NIR}{RED}-1}{\frac{NIR}{RED}} \tag{2}$$

The NDVI value oscillates between − 1 and 1 (Fig. 5) where the positive values (green) prove the existence of vegetation areas and the negative ones (red) are evidence of non-vegetative features (water, barren lands, clouds and snow).

NDWI

The Normalized Difference Water Index (NDWI) is considered as a crucial tool in monitoring and delineating open water features using remotely sensed data (as defined by Gao (1996) in Eq. (3) and McFeeters (1996) in Eq. (4)). The NDWI can be helpful in improving agriculture by controlling irrigation in real time. Hence, it helps prevent severe damage to the crops especially in water-stressed areas such as the one considered in our case study.

$$NDWI = \frac{\mathrm{NIR}-\mathrm{SWIR}}{\mathrm{NIR}+\mathrm{SWIR}} \tag{3}$$

$$NDWI = \frac{\mathrm{GREEN}-\mathrm{NIR}}{\mathrm{GREEN}+\mathrm{NIR}} \tag{4}$$

As depicted in Fig. 6, high NDWI values (blue) correspond to high plant water content and water features. Low NDWI values (green) correspond to low or non-vegetation content or non-water bodies.

Change detection

Change detection is a process applied to identify, monitor and manage differences of an object through a specific period. It provides a quantitative analysis of temporal phenomena based on multi-date satellite imagery. It has been suitable for diverse fields, from land use change analysis to the assessment of crops quality and quantity (phenology, production, stress), covering even the study of environmental changes and natural disaster monitoring (snow melt, daily thermal characteristics) (Cohen 1960; Singh 1989).

Change detection is a vulnerable process because accuracy is too sensitive to enormous errors due to the seasonal differences made by the vegetation phenology cycle. Other errors originate from sensor differences when they are partly minimized, in case of Landsat file, by holding the sensor system. For this purpose, preventive actions have to be undertaken especially by reviewing for any existent confusion between detected changes and potential errors (Dai 1998). The importance of change detection has been increasing remarkably over the past few decades notably in environmental resources management. It generally requires remote sensing data to provide quantitative and timely information exhibited in 'from _ to' change information of land cover through a cross-tabulation matrix.

In this case study, the outcome of change detection analysis was expressed through a cross-tabulation matrix. The matrix described the LULC change made from 2002 to 2018 images. The purpose was to understand major changes that occurred from one class to another through the study period. Conversion changes from all the classes of 2002 through 2018 were illustrated in a change detection map (Fig. 4).

A cross-tabulation matrix was accomplished by IDRISSI SELVA via the CROSSTAB tool. This procedure generally required earlier (2002) and later (2018) classified images to study class interactions during that period.

Weather data

In order to study the weather behaviour of our watershed, we have collected climate data for different stations located within the watershed (Fig. 1). The data were used by AQUACROP software. It is an open-source software developed by FAO to understand the effect of the environment and soils on crop production. At this stage, we would stop at the point of studying the effect of climate change based on the following historical weather data:

- Daily maximum (Tmax) and minimum (Tmin) temperature (°C).
- Daily rainfall (P) data (mm) of 2002 and 2018.
- Wind speed (m/s) data measured at 2 m above the soil surface.
- Daily relative humidity (fraction) known as vapour pressure deficit or saturation deficit.
- Solar energy (MJ/m^2) or radiation data are either measured directly with a radiometre or can be estimated based on the actual duration of sunshine using the Campbell-Stokes sunshine recorder.
- The station location (latitude and elevation) is also required to compute the day length and extra-terrestrial radiation.

Outputs of AQUACROP

For each day of the simulation period, AQUACROP requires the historical weather climate data mentioned in the previous section. It computes the following:

- The reference evapotranspiration (ET0): The main purpose of ET0 is to assess the evaporative demand of the atmosphere based on weather data only. In AQUACROP, ET0 is computed according to the FAO Penman-Monteith equation given as follows:

$$ET0\ (\mathrm{mm/day}) = \frac{0.408\Delta(\mathrm{Rn}-\mathrm{G}) + \Upsilon \frac{900}{T+273}\,\mathrm{U2}\,(\mathrm{es}-ea)}{\Delta + \Upsilon(1+0.34\mathrm{U2})} \quad (5)$$

where:
*R*n net radiation at the crop surface [MJ m-2 day-1],
G soil heat flux density [MJ m-2 day-1],
T air temperature at 2 m height [°C],
*U*2 wind speed at 2 m height [m s-1],
es saturation vapour pressure [kPa],
ea actual vapour pressure [kPa],
es − ea. saturation vapour pressure deficit [kPa],
Δ slope vapour pressure curve [kPa °C-1],
ϒ psychrometric constant [kPa °C-1].

- Rainfall data (*P*): rainfall data are presented either monthly or annually. Rainfall data are essential for AQUACROP to calculate soil water balance.
- Average T_{min} and T_{max}: average T_{min} and T_{max} are presented in °C. In fact, these parameters can influence ET0 because air can easily transfer the heat energy to the crops.
- Growing degree days (GDD): it is defined as the required mean temperature (average daily minimum and

maximum temperatures) and days for the crop to reach maturity.

Results and discussion

Supervised classification was operated for 2002 and 2018 images using the maximum likelihood classifier. Both classified maps are illustrated in Figs. 2 and 3. The result of the CROSSTAB operation is represented in 2002 to 2018 change detection map (Fig. 4) accompanied by a cross-tabulation matrix (Table 4). The coupling of the overall classification accuracy and kappa statistics reveals 86.9%/0.78 and 88.1%/0.85 respectively for 2002 and 2018 classification images (Table 5). According to Anderson et al. (1976), the minimum tolerated accuracy assessment should not be less than 85% which is acceptable in our case. Regarding the Kappa statistics, they were compared based on the classification of Landis and Koch (1977) making it a reliable tool for evaluation. Both components seem to be convenient according to the above-mentioned conventional standards.

During the classification process, most problems generally occur because of possible confusion between urban areas, bare grounds and especially between some of the agricultural lands as it is often hard to distinguish olive from viticulture and arboriculture. For this reason, a post-classification field visit is essential for necessary corrections using the GIS tool. These similarities are responsible for the regression of the overall accuracy and kappa index. Selecting ground truth areas is directly linked to altering or enhancing the classification process. In fact, reassembling the sampled areas is the most difficult and delicate aspect for image classification (Paola and Schowengerdt 1995). Classification results for 2002 and 2018 are summarized in Table 6 which displays the exact percentage of land use classes. Based on these results, it seems that some major changes have occurred during that study period.

Olive and viticulture

The increase in olive lands is a characteristic development, especially in Tunisia. Almost 30% of the Tunisian lands are dedicated for olive growing. In fact, FAO (2015) has cited in 2012 that 1.76 million hectares were devoted for olive cultivation. Tunisia is considered a leader in olive oil production and exportation (Tunisian Republic, Ministry of Industry 2016).

In 2012, Tunisia produced 170,000 tons of olives. It is classified as the fourth, and sixth in non-productive cycles, world leader in producing oil olive. For that considerable amount of production, the country is well-known as the third exporter of olive oil in the world behind Spain and Italy. This resulted in the fact that olive oil represents 10% of Tunisia's agricultural production. Almost 30 to 40% of agricultural exportation consists of olive oil which represents 2% of the gross domestic product (GDP). Additionally, 17% of agriculture activities are dedicated for olives. All this attests to the fact that the Tunisian economy relies on olive cultivation, which explains the encouraging strategies the Tunisian government is undertaking to motivate farmers for olive growing (FAO 2015a).

The Algerian economy is rather based on both olive cultivation and viticulture. Algeria has dedicated over 29,000,000 ha to olive cultivation. On the other hand, viticulture farming is also another growing agricultural alternative. The dedicated lands to this activity have almost doubled increasing from 515,000 ha in 2000 to over 1,000,000 ha in 2006 (INRAA 2007). Additionally, more than 396,000 ha of viticulture are devoted for wine industries which makes Algeria the second-largest wine producer and the fifth wine exporter in Africa (Isnard 1975; HuffPost Algérie 2015).

Arboriculture

This class has gone through a dramatic decrease during the study period from 952.21 km^2 in 2002 to 619 km^2 in 2018. In fact, the exportation of Tunisia's arboriculture has been decreasing over the last decade due to the decline of arboriculture lands (Houssem Eddine CHEBBI et al. 2019). The encouraging strategies in Tunisia to increase olive production are being seriously applied (FAO 2015a), which has reciprocally affected the arboriculture. Many farmers have converted their lands from arboriculture lands to olive trees. The Mediterranean climate is also a major factor since it is perfectly adequate for olive culture. As for Algeria, arboriculture lands are still very low and barely represent 3% of the total agricultural lands (flehetna.com 2018).

Urban area

The urban area has increased noticeably from 65.5 km^2 (0.58%) to 268.6 km^2 (2.5%). Urban expansion is generally associated with the demographic development of the area. On the one hand, the Algerian population has grown from 32 million in 2002 to 42 million in 2018 (Université de Sherbrooke - Québec - Canada 2020). Yet, in 2018, Algeria registered over one million births compared with 589,000 in 2002 (LIBERTE-ALGERIE.COM, 2019). On the other hand, the Tunisian population has grown from almost 10 million in 2002 to 11.5 million in 2018 (Université de Sherbrooke - Québec - Canada 2020). This fact explains the urban expansion in the study area which led to the increasing demand for food supplies manifested mainly in the expansion of agricultural lands (except for the arboriculture).

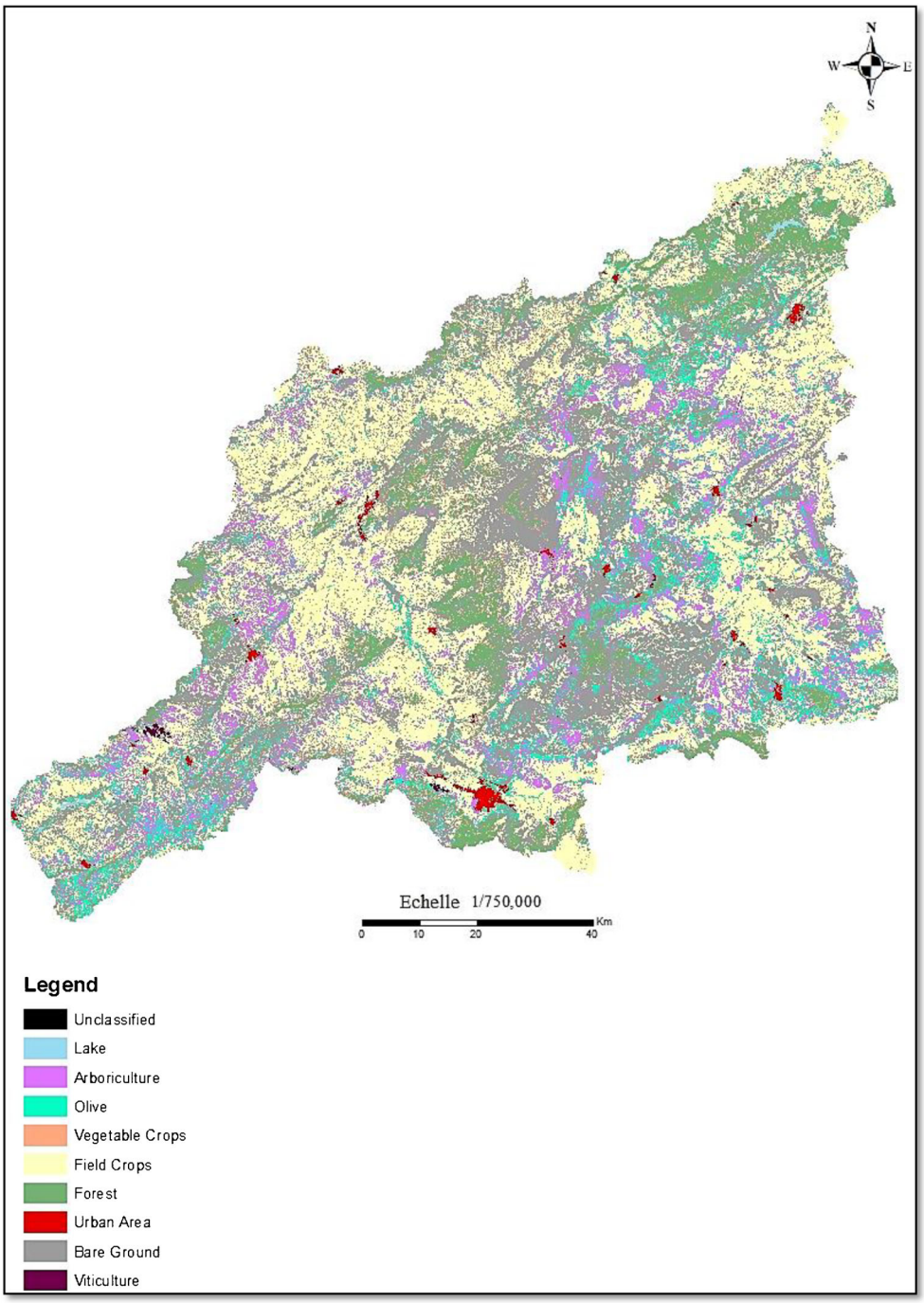

Fig. 2 LULC classification map of 2002

Field crops and vegetable crops

Field crops have expanded from 4507 km^2 in 2002 to 5051 km^2 in 2018 and those devoted to vegetable crops have increased from 372 km^2 in 2002 to 549 km^2 in 2018. In fact, Algeria achieved a significant increase (62%) of cereal production to reach over 4.2 million tons (from 2011 to 2015) but it recorded only 2.6 million tons (from 1995 to 1999). A sharp rise of 400% in the production of vegetable crops was also achieved, jumping from 3.23 million tons (from 1995 to 1999) to 15.8 million tons (from 2011 to 2015) (Harbouze et al. 2019).

Tunisia has also noticed a significant increase in cereal production at an annual average of 2.51%/year for a study period ranging from 2003 to 2014. Further, vegetable production has improved, and vegetable exports have reached 56,000 tons in 2013/2014 while it was only 12,058 tons in 2003/2004 (République Tunisienne, Ministère de l'Agriculture et des Ressources Hydrauliques et de la Pêche, 2015). Consequently, vegetable-based processed product

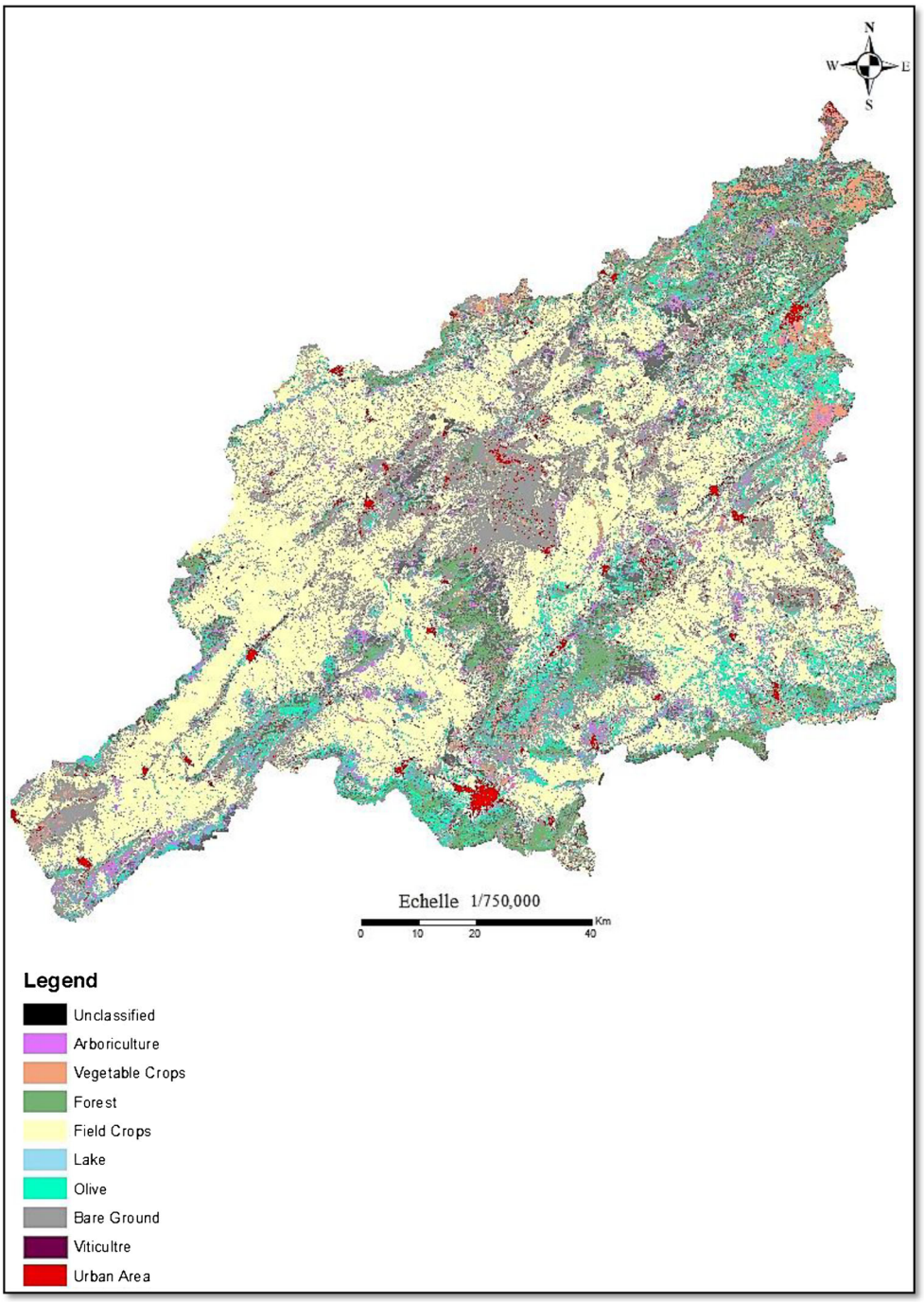

Fig. 3 LULC classification map of 2018

production and exportation are increasing, as well to satisfy both local and world needs (UTICA-TUNISIE 2011).

Forest

This class has decreased from 741 km^2 in 2002 to 532 km^2 in 2018. This issue seems to be the whole world concern. Forests are threatened by irresponsible deforestation and fires. Despite the considerable efforts of both countries (Algeria and Tunisia) in the afforestation, further actions are still required. Figure 5 shows interpreted NDVI images for 2002 and 2018. We can clearly observe the remarkable degradation of forests especially in the upper part of the catchment. In Tunisia, the socio-political status of the country since 2011 (revolution) has badly affected the forest sector. Deforestation was not been indicated in Tunisian forests for the last statistics of FAO due to these socio-economic issues. Yet, over 400,000 m^3 of wood have been produced from Tunisian

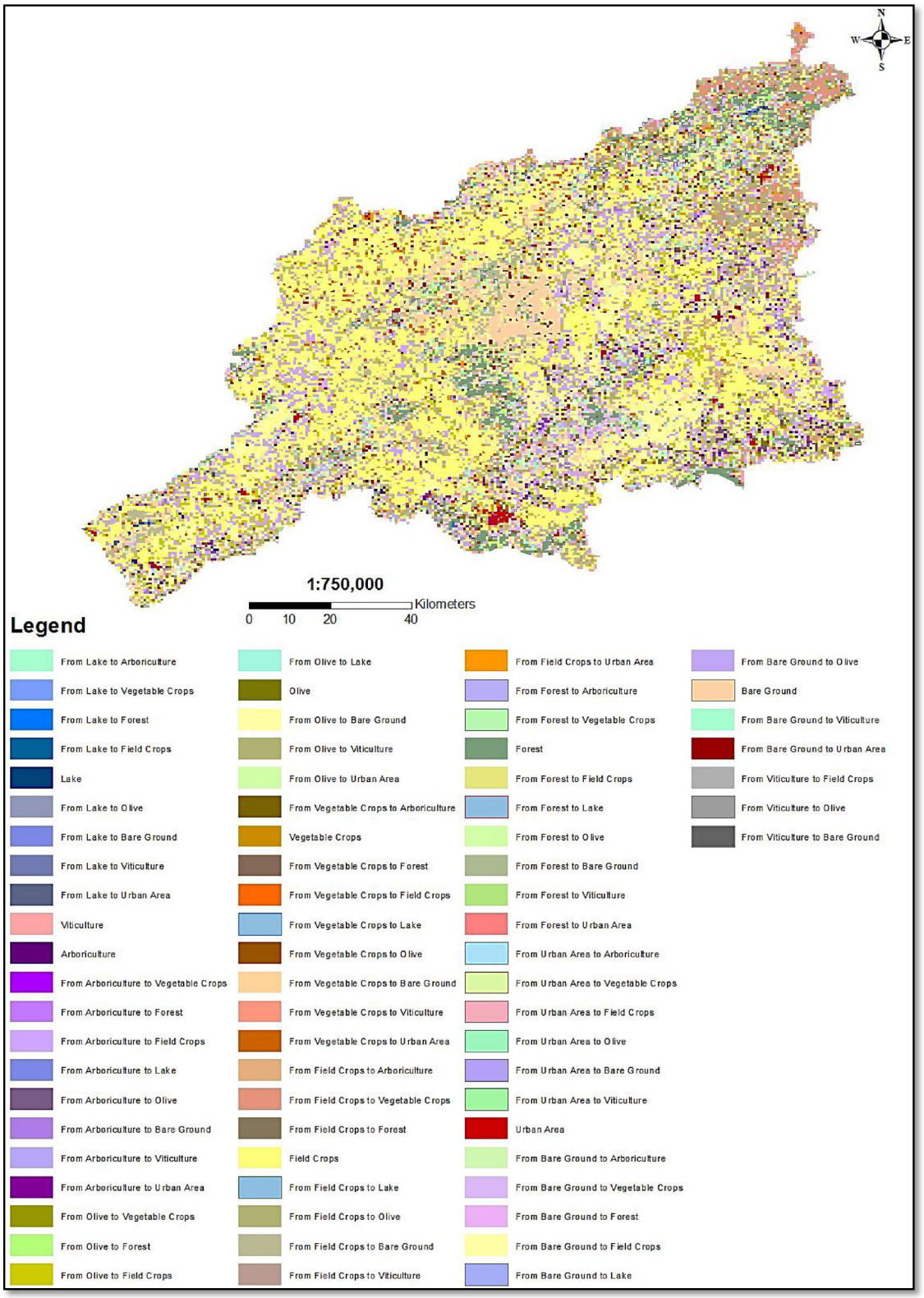

Fig. 4 Land use change detection from 2002 to 2018

forests (Chriha and Sghari 2013; FAO 2015b). In Algeria, deforestation has intensified recording an increase from 11,000 ha/year in 2005 up to 18,000 ha/year in 2018 (FAO 2015c).

Table 4 Cross-Tabulation matrix between 2002 and 2018

Class	2002										
2018	Unclassified	Lake	Arboriculture	Olive	Vegetable crops	Field Crops	Forest	Urban Area	Bare Ground	Viticulture	Total
Unclassified	7.16	0.00	0.00	0.00	0.00	0.00	0.00	0.00	0.00	0.00	7.16
Arboriculture	0.00	1.95	48.85	80.11	20.52	233.49	51.13	0.65	182.37	0.00	619.07
Vegetable crops	0.00	0.65	9.77	37.78	21.17	280.71	37.12	0.65	161.20	0.00	549.05
Forest	0.00	0.65	0.98	26.70	31.26	37.12	321.75	0.00	114.30	0.00	532.77
Field crops	0.00	3.26	629.81	357.89	142.96	2719.86	41.03	6.51	1143.37	7.16	5051.86
Lake	0.00	0.98	0.98	1.95	1.30	7.49	1.63	0.00	4.88	0.00	19.21
Olive	0.00	1.95	87.60	130.91	37.12	433.12	61.55	5.21	283.97	0.65	1042.09
Bare ground	0.00	2.93	132.54	151.10	83.04	632.42	113.65	11.40	912.15	2.93	2042.17
Viticulture	0.00	1.30	5.86	38.43	27.35	106.16	106.81	0.65	125.38	0.00	411.95
Urban area	0.00	2.61	35.82	25.40	8.14	56.99	6.51	36.47	96.72	0.00	268.66
Total	7.16	16.28	952.21	850.28	372.87	4507.37	741.19	61.55	3024.34	10.75	10,544.0

Bare ground

This class has decreased from 3024.34 km^2 in 2002 to 2042.17 km^2 in 2018. Considering that the total area is always unchangeable (10,544 km^2), the increase of some classes area automatically leads to the decrease of the others and bare grounds seem to the one that suffers. The decline of bare ground areas can be explained by several factors. First, the expansion of the urban area has caused areas of bare ground to be converted into new urban settlements. Some of the converted bare lands have been reused in agriculture especially in field crops and olive trees. Moreover, late statistics have indicated that olive lands occupied 45% of the total arable lands in Tunisia (FAO 2015a).

Lakes and water resources

Although there are no big changes in lakes during the study period (from 16 km^2 in 2002 to 19 km^2 in 2018), other factors indicate that the water resources are being intensively used. To begin with, the expansion of agricultural lands (olive, field crops and vegetable crops) would result in the rise of the need for water for irrigation. More than 500,000 ha have been added to agricultural lands in 2014 compared with those in 1994. Algeria has been unprecedentedly using shallow and deep water. The number of dams has increased from 44 with a storage capacity of 3.3 billion m^3 in 1994 up to 100 dams in 2016 with a mobility water storage of 12 billion m^3. Half of that water capacity is dedicated to agriculture and irrigation (6 billion m^3). Irrigated land area has increased from 350,000 ha in 2000 up to 1.3 million ha in 2017 (Harbouze et al. 2019). On the other hand, Tunisia is threatened by water scarcity due to the shortage of water surfaces and the intensification of arid climate. The expansion of the irrigated lands (from 380,000 ha in 2001 up to 460,000 ha in 2010) will automatically require extra amounts of water supplies. This fact has led to the

Table 5 Overall accuracy and Kappa coefficient statistics for 2002 and 2018 classified maps

Classified image	Overall accuracy (%)	Kappa coefficient
2002	86.9103	0.7837
2018	88.1442	0.8489

Table 6 Area and percentage of land use classes of 2002 and 2018 map

Year	2002		2018	
Class	Area (km^2)	%	Area (km^2)	%
Lake	16.28	0.15	19.21	0.18
Arboriculture	952.21	9.03	619.07	5.87
Olive	850.28	8.06	1042.09	9.88
Vegetable crops	372.87	3.54	549.05	5.20
Field crops	4507.37	42.76	5051.86	47.90
Forest	741.19	7.03	532.77	5.05
Urban area	61.55	0.58	268.66	2.55
Bare ground	3024.34	28.68	2042.17	19.39
Viticulture	10.75	0.10	411.95	3.91
Unclassified	7.16	0.07	7.16	0.07
Total	10,544	100.00	10,544	100.00

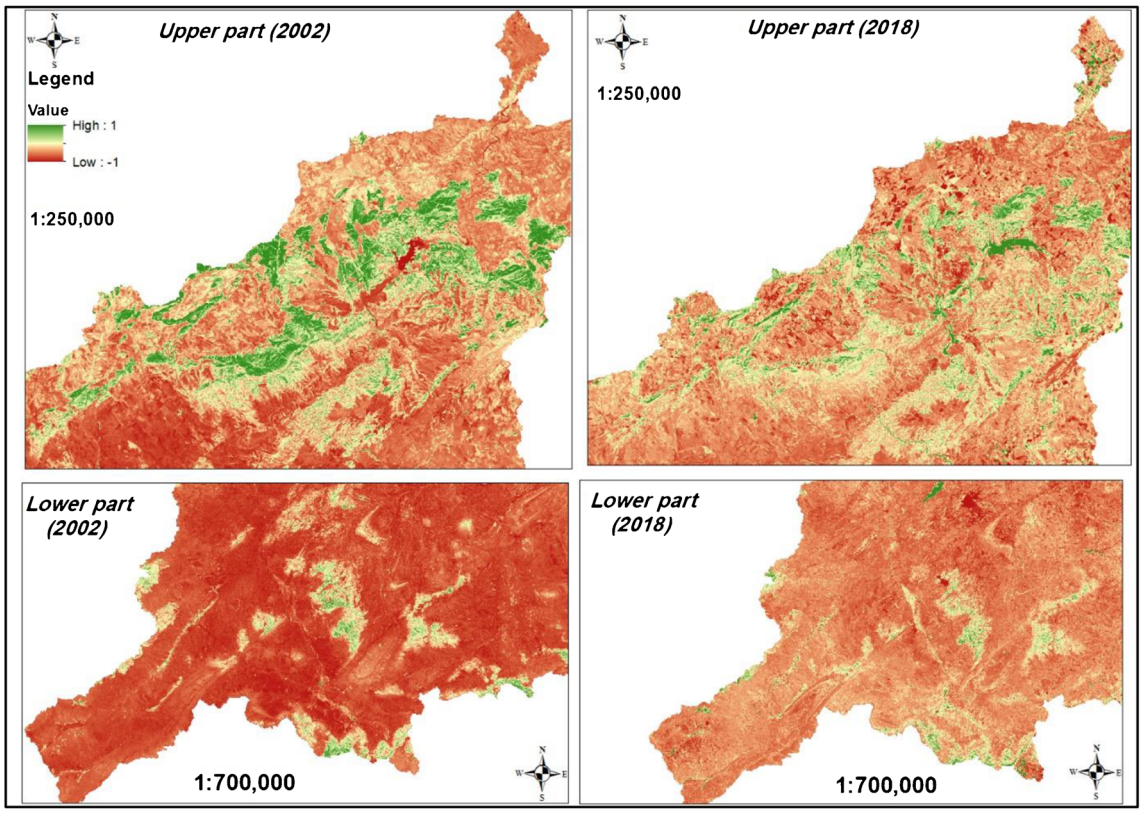

Fig. 5 Comparative NDVI images (2002 and 2018) for the upper and lower parts of Mellegue catchment

excessive use of shallow and deep water, altered water quality and increased salinity (Laajimi 2011; Chebbi et al. 2019). Tunisia and Algeria are still under the low average of hydric stress (500 m3 / habitant/ an) with high baseline water stress (Hofste et al. 2019). We can forecast that with the demographic growth, the demand for water supplies will be intensified.

Figure 1 shows the location of the Mellegue Dam, serving the approximate cities with irrigation and drinking water. In the last couple of years, a serious decrease in water resources has been noticed. Figure 6 shows NDWI for both 2002 and 2018 satellite images. We can clearly notice a serious degradation of the water resources of the dam. Moreover, the maximum water storage of the dam has dropped to 1/3 compared with its initial capacity. Water salinity has increased, and more than half of the dam was silted. In fact, a recent study has mentioned that the dam will be entirely silted by 2025 (Cherni et al. 2010). Based on water storage data of the dam during the study period, we were able to produce two predictable models (Fig. 7): The first one (using Excel) is based on the exponential behaviour of the real data curve (bleu). The model (red) can affirm that the dam can no longer store water by the end of 2027 which will lead to the previous assumption that the dam will be totally silted. The second model, however, was built using the R program. The model has employed time series function so we can determine the perfect Autoregressive integrated moving average (ARIMA) model, using AUTO.ARIMA function, for future forecasting. We concluded that the best ARIMA model will be (0,1,0), meaning a random walk model with a minimum slow mean reversion. As we can see, the future contribution of the dam (blue) will be very low (close to zero). Figure 8 illustrates a zoomed portion of 2002 and 2018 LULC classified images (only lakes) for the water occupation in the dam. The clear decrease in water storage can be clearly observed, and Fig. 9 confirms this interpretation. It represents comparative histograms of the water resources of the dam between 2002 and 2018 (Ministère de L'Agriculture 2019). Even though there is no big difference in precipitation between the two dates (Fig. 9), the dam water storage has severely declined from 68 million m^3 in 2002 to only 5 million m^3. This fact was also supported by the contribution of the dam in irrigated and drinking water, which has also declined from 292 million m^3 in 2002 to settle at 6 million m^3 in 2018. Based on these figures we can confirm the alarming state of the water resources of the watershed which is mainly due to the urban area expansion, excessive use and demand for water (for irrigation as for industries) and poor management strategies for water preservation.

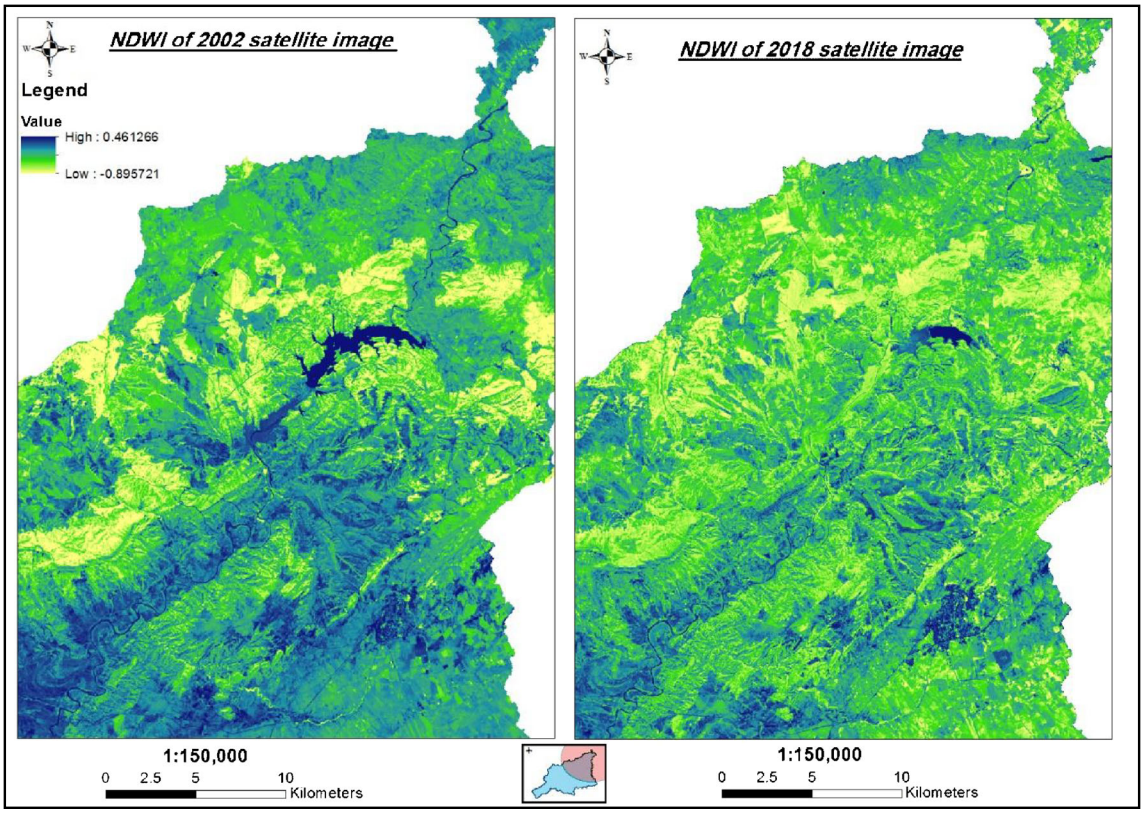

Fig. 6 Comparative NDWI images (2002 and 2018) for the upper part of Mellegue catchment

Impact of LULC changes on the catchment weather

*T*min and *T*max

The output of the simulation (Figs. 10 and 11) reveals that there is a general decrease in both *T*max and *T*min with some exceptions (stations 7 and 14) especially in station 28 where there is a little increase of 1 to 2 °C. These changes are based on two major factors: First the external temperature (*T*max and *T*min) decreases due to the conversion of bare ground which may cause an increase of surface temperature owing to their great reflectance. Second, temperature decrease is also known to be due to the high biomass/vegetative land use (Weng et al. 2004; Youneszadeh et al. 2015) which applies to our study case study where there is a noticeable extension of agricultural lands (olive, viticulture, vegetable and field crops). Station 28, belonging to the upper part of the catchment, has undergone the main increase in temperature accompanied by a decline of forest areas based on

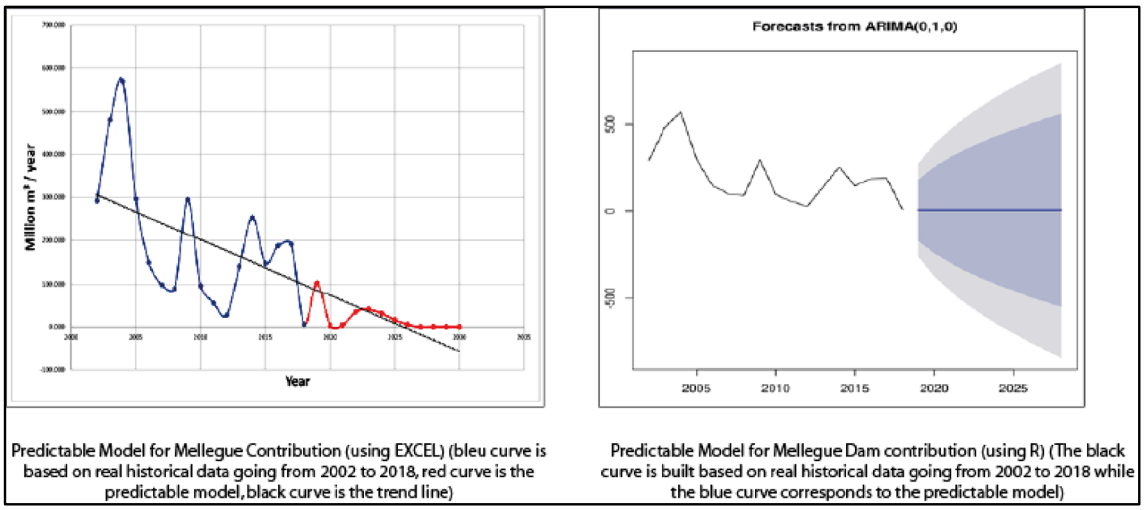

Fig. 7 Predictable models for Mellegue contribution

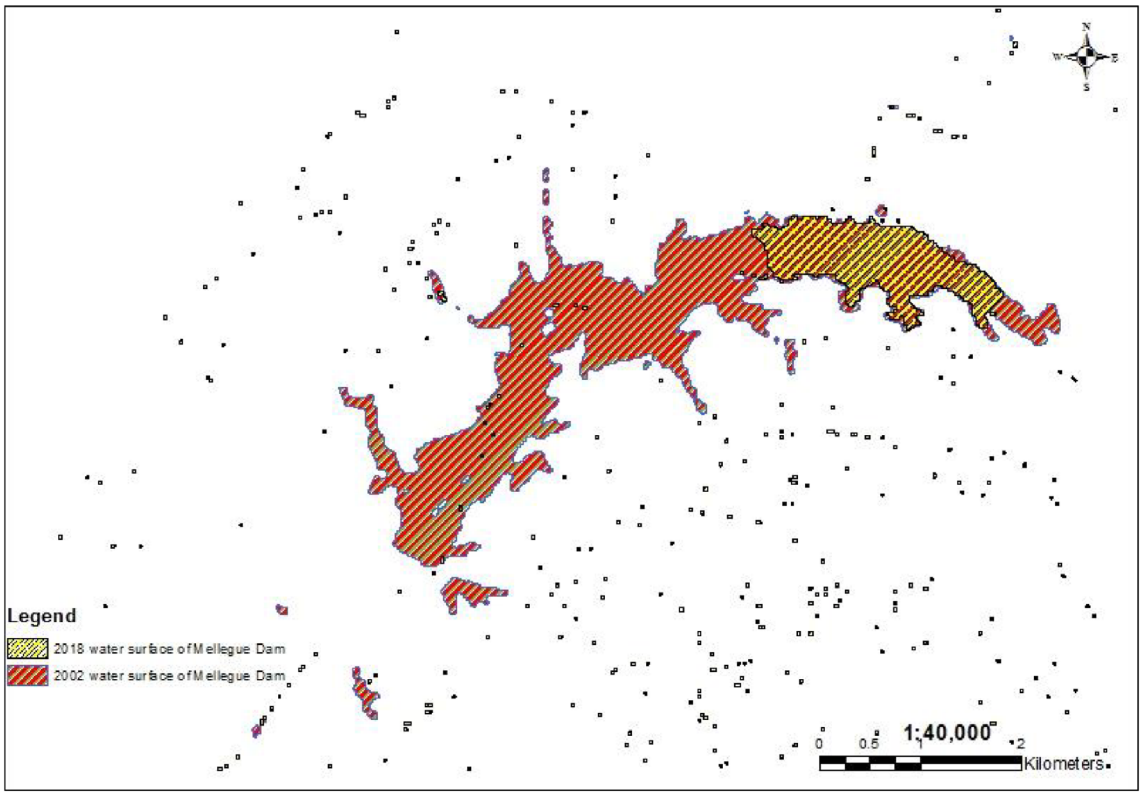

Fig. 8 Supervised classification of the Mellegue dam based on 2002 and 2018 satellite images

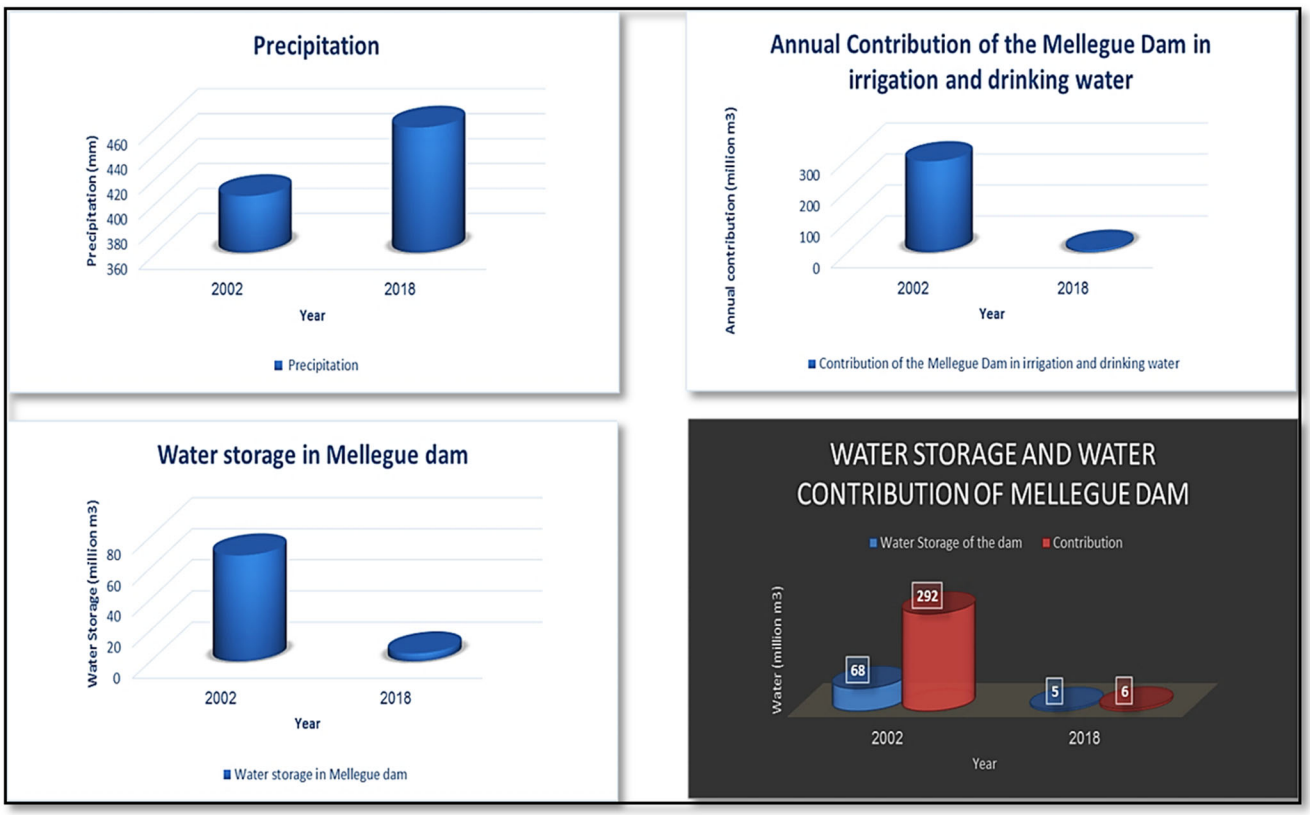

Fig. 9 Precipitation, water storage and contribution of Mellegue dam

the NDVI observation. Here, the increase of temperature is also due to the extension of built-up areas (Sentian and Kong 2015; Singh et al. 2017; Niu et al. 2018).

ET0

Based on the ET0 maps (Figs. 10 and 11), we may conclude that the catchment is divided into two major parts. In the first part (the lower one), we distinguish an ET0 decrease at an average of 100 mm/year. In the second part (the upper one), we can see an ET0 increase of 50 mm/year to 140 mm/year. Based on the equation of Penman-Monteith for reference evaporation (ET0), it is very common that the ET0 trend is the same as the external temperature graphs (*T*min and *T*max). Despite the potential decline of relative humidity (Rh) due to the expansion of vegetative lands, the only factors that may contribute to the ET0 decrease are still external temperatures and wind speed (Wang et al. 2012). However, the expansion of urban areas, along with the decrease of forests are responsible for the increasing ET0 mainly noticed in the upper part of the catchment (Yang et al. 2012; Li et al. 2017).

Rainfall (*P*)

Based on the revealed weather data shown in Figs. 10 and 11, we can observe the complex behaviour of precipitation during the study period. Several potential factors can be responsible for this rainfall fluctuation. Urbanized areas are considered as the main reason of increasing precipitation and downwind. They are also the origin of the settlement of thunderstorms along with the freezing weather and heavy rain due to the phenomenon of Urban Heat Island (UHI) (Pielke et al. 2007; Xie et al. 2014). Moreover, water management can be difficult because it seems that artificial waterproofs of the urbanized area are reducing water infiltration leading, therefore, to the shrinking of groundwater recharges. Nonetheless, the runoff is very high in urbanized areas due to these artificial grounds which might be linked to the initiation of floods. Furthermore, irrigated lands can intervene on the fluctuation of the precipitation process and play a part in reducing the water and causing a potential drought as a result, besides increasing the runoffs (Pielke et al. 2007; Dong et al. 2015). Another essential reason is closely tied to the degradation of forests, which can be responsible for the reduction of cloud condensation and intensification of soil evaporation along with the reduction in transpiration, affecting moisture availability. Finally, even the unused lands can be linked to the fluctuating runoff rate (Pielke et al. 2007; Li et al. 2018).

GDD

Computed GDD is based on the following equation:

$$GDD = \sum_{i}^{365} \left(\frac{Td\ (i)\max - td(i)\min}{2} - Td(\text{base}) \right) \quad (6)$$

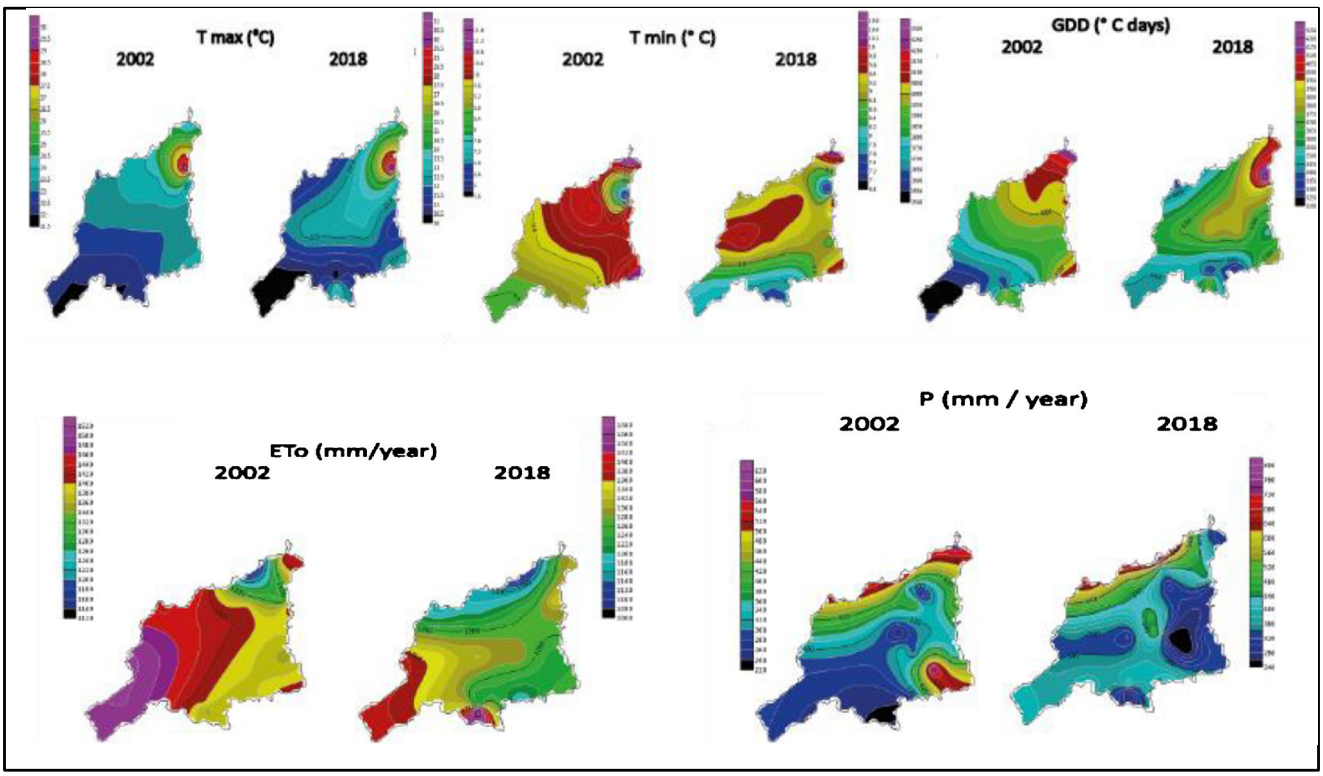

Fig. 10 Weather maps of Mellegue catchment for 2002 and 2018

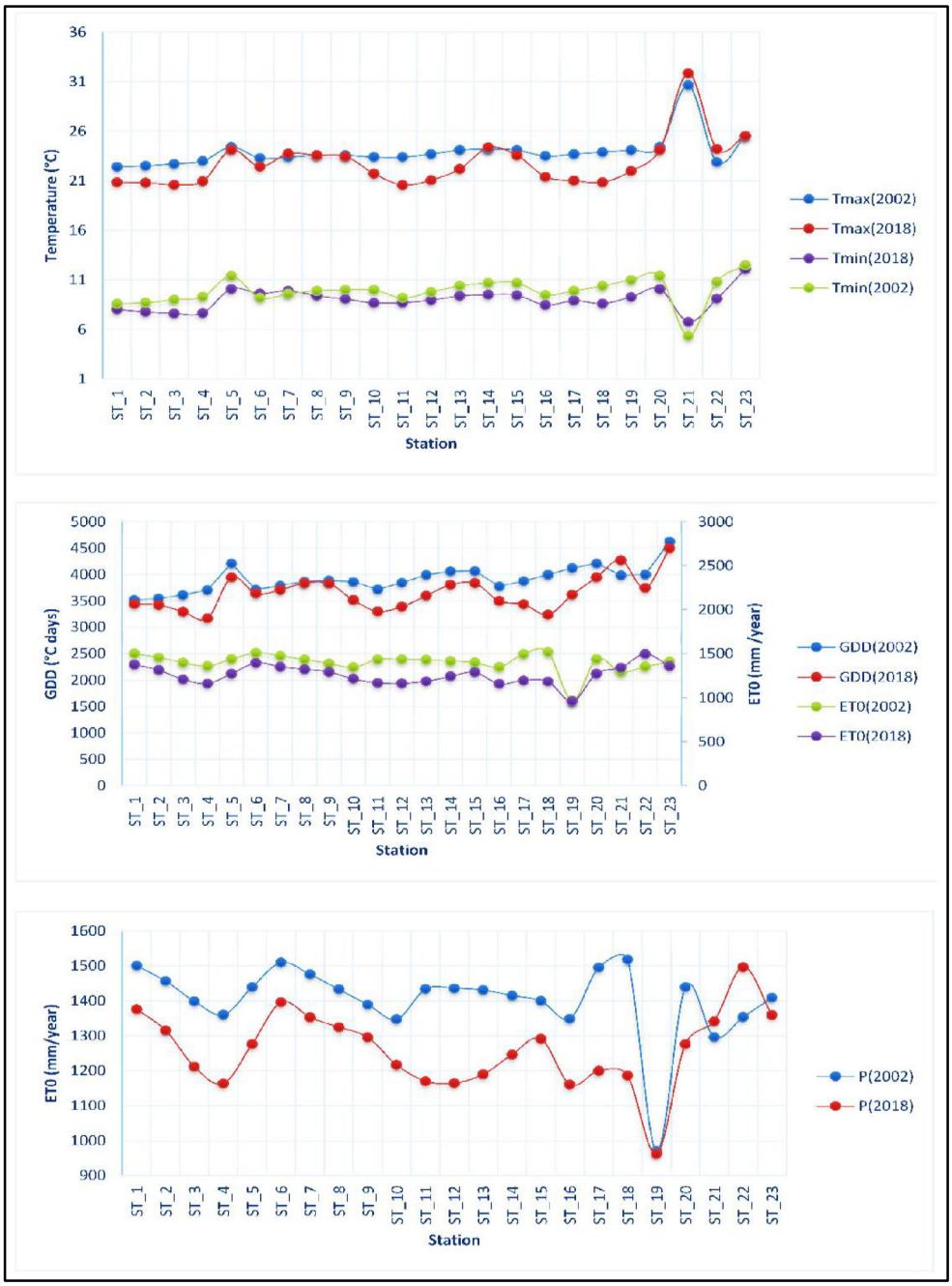

Fig. 11 Weather data of Mellegue catchment for 2002 and 2018

GDD: accumulated growing degree-day,*Td* (*i*) max: Maximum temperature,*Td* (*i*) min: Minimum temperature,*Td* (base): base temperature and known as 5 °C

As seen, the GDD exclusively depends on external temperatures. So, based on the Figs. 10 and 11, we can remark that the GDD of 2018 is lower than that of 2002 except for Station 21, which has the same Tmin and Tmax trend. Even though some researchers suggest that LULC changes could intervene indirectly in GDD (Zhang et al. 2019), this still needs further studies to prove while considering other factors like weather and crop type.

Conclusion

The main objective of this research was to evaluate the spatial distribution of LULC change through a specific period (from 2002 to 2018). It needed remote sensing tools relying on a supervised classification process with the maximum likelihood classifier. It also applied a visual interpretation and ground truth data using the GIS tool which plays a central role in enhancing the accuracy assessment of the maps classification.

According to the classification results, it was found that a considerable increase was noticed in agricultural lands mainly seen in olive trees, field crops, vegetable crops and viticulture. Increases in these lands were mainly the result of urban expansion. Economic prosperity hit the region because of these modifications. In addition, due to excessive demand for food following demographic growth, new strategies have been implemented in the development of irrigated lands in order to improve crop productivity. Increases of these lands have led to the shrinking of others. The major threat is embodied in the decrease of forests although they play a vital role in cleaning the air from pollution and preserving the ecosystems. The urban expansion has required additional water quantities, which caused an irreversible serious decrease in the river resources. This fact was intensified by the development of irrigated lands and industries. The degradation of water quality was caused by industries that grew along with urban expansion. In addition, built-up areas are reducing the water infiltration phenomenon which naturally contributes to refilling underground water resources. As a result, the decrease of infiltration automatically led to an increase in runoff and may consequently initiate floods that could damage agricultural crops and decrease yields capacity. Preventive measures have to be taken in order to preserve the ecosystem and life sustainability. These can be cited as follows:

- Development of new strategies for saving superficial water intended for ulterior use and reducing the exploitation of underground water supplies.
- Considering new alternatives for saving water resources like seawater desalination and reuse of recycled water.
- Continuous yearly afforestation actions to reduce erosion, desertification and air pollution.
- Governmental cooperation between Tunisia and Algeria in order to restore degraded lands like soils, forests and especially water like planning for a new management strategy that may help reduce these negative impacts on the environment and the ecosystem.

References4

Ahmadizadeh S, Yousefi M, Saghafi M (2014) Land use change detection using remote sensing and artificial neural network : application to Birjand, Iran. 4:276–288

Anderson JR, Hardy EE, Roach JT, Witmer RE (1976) A land use and land cover classification system for use with remote sensor data

Araya YH, Cabral P (2010) Analysis and modeling of urban land cover change in Setúbal and Sesimbra, Portugal. Remote Sens 2:1549–1563. https://doi.org/10.3390/rs2061549

Baynard CW (2013) Remote Sensing Applications: Beyond Land-Use and Land-Cover Change. 2013:228–241

Becker F, Choudhury BJ (1988) Relative sensitivity of normalized difference vegetation index (NDVI) and microwave polarization difference index (MPDI) for vegetation and desertification monitoring. Remote Sens Environ 24:297–311. https://doi.org/10.1016/0034-4257(88)90031-4

Belloula M, Dridi H (2015) Modeling of the flows and solid transport in the catchment area of Meskiana-Mellegue upstream (northeastern Algeria). Geogr Tech 10:1–7

Berberoglu S, Akin A (2009) Assessing different remote sensing techniques to detect land use/cover changes in the eastern Mediterranean. Int J Appl Earth Obs Geoinf 11:46–53. https://doi.org/10.1016/j.jag.2008.06.002

Biswas AK (1990) Watershed management. Int J Water Resour Dev 6:240–249. https://doi.org/10.1080/07900629008722479

Bronstert A, Niehoff D, Brger G (2002) Effects of climate and land-use change on storm runoff generation: present knowledge and modelling capabilities. Hydrol Process 16:509–529. https://doi.org/10.1002/hyp.326

Chebbi H., Pellissier J-P, Khechimi W, Rolland J-P (2019) Rapport de synthèse sur l'agriculture en Tunisie

CHERNI S, KHLIFI S, LOUATI MH (2010) SUIVI DE L'ENVASEMENT DE LA RETENUE DU BARRAGE DE NEBEUR SUR L'OUED MELLEGUE (LE KEF). In: Actes des 17èmes Journées Scientifiques sur les Résultats de la Recherche Agricoles

CHRIHA S, SGHARI A (2013) Forest fires in Tunisia, irreversible sequelae of the revolution of 2011. J Mediterr Geogr 121

Cohen J (1960) A coefficient of agreement for nominal scales. Educ Psychol Meas 20:37–46. https://doi.org/10.1177/001316446002000104

Dai X (1998) The effects of image misregistration on the accuracy of remotely sensed change detection. IEEE Trans Geosci Remote Sens 36:1566–1577. https://doi.org/10.1109/36.718860

Dewan AM, Yamaguchi Y (2009) Land use and land cover change in greater Dhaka, Bangladesh: using remote sensing to promote sustainable urbanization. Appl Geogr 29:390–401. https://doi.org/10.1016/j.apgeog.2008.12.005

Dong L, Xiong L, Lall U, Wang J (2015) The effects of land use change and precipitation change on direct runoff in Wei River watershed, China. Water Sci Technol 71:289–295. https://doi.org/10.2166/wst.2014.510

FAO (2015a) Analyse de la filière oléicole

FAO (2015b) Evaluation Des Ressources Forestieres Mondiales 2015 - TUNISIE

FAO (2015c) Evaluation Des Ressources Forestieres Mondiales 2015 - Algérie

Fohrer N, Haverkamp S, Eckhardt K, Frede H-G (2001) Hydrologic response to land use changes on the catchment scale. Pergamon Phys Chem Earth (B) 26:577–582. https://doi.org/10.1016/S1464-1909(01)00052-1

Gao BC (1996) NDWI - a normalized difference water index for remote sensing of vegetation liquid water from space. Remote Sens Environ 58:257–266. https://doi.org/10.1016/S0034-4257(96)00067-3

Gómez D, Montero J (2011) Determining the accuracy in image supervised classification problems. In: Proceedings of the 7th conference of the European Society for Fuzzy Logic and Technology (EUSFLAT-11). Atlantis Press, pp 342–349

Harbouze R, Pellissier J-P, Rolland J-P, Khechimi W (2019) Rapport de synthèse sur l'agriculture en Algérie

Hofste RW, Reig P, Schleifer L (2019) 17 countries, home to one-quarter of the world's population, face extremely high water stress. World Resour Inst 1

HuffPost Algérie (2015) L'Algérie 2e producteur, 5e exportateur de vin en Afrique et 11e consommateur au monde | Al HuffPost Maghreb. https://www.huffpostmaghreb.com/2015/09/05/algerie-vigne_n_8092750.html.

INRAA (2007) Rapport national sur l'état des ressources phytogénétiques pour l'alimentation et l'agriculture 44

Isnard H (1975) La viticulture algérienne, colonisation et décolonisation. Méditerranée 23:3–10. https://doi.org/10.3406/medit.1975.1635

J.A. Rodier, J. Colombani, J. Claude, R. Kallel (1981) Le Bassin De La Mejerdah

Johnes P, Heathwaite A (1997) Modelling the impact of land use change on water quality in agricultural catchments. Hydrol Process 11:269–286. https://doi.org/10.1002/(sici)1099-1085(19970315)11:3<269::aid-hyp442>3.0.co;2-k

Kumar N, Tischbein B, Kusche J, Laux P, Beg MK, Bogardi JJ (2017) Impact of climate change on water resources of upper Kharun catchment in Chhattisgarh, India. J Hydrol Reg Stud 13:189–207. https://doi.org/10.1016/j.ejrh.2017.07.008

Laajimi A (2011) Les périmètres irrigués en Tunisie Un enjeu pour le développement de la production agricole

Landis JR, Koch GG (1977) The measurement of observer agreement for categorical data. Biometrics 33:159–174. https://doi.org/10.2307/2529310

Li BQ, Xiao WH, Wang YC, Yang MZ, Huang Y (2018) Impact of land use/cover change on the relationship between precipitation and runoff in typical area. J Water Clim Chang 9:261–274. https://doi.org/10.2166/wcc.2018.055

Li G, Zhang F, Jing Y, Liu Y, Sun G (2017) Response of evapotranspiration to changes in land use and land cover and climate in China during 2001–2013. Sci Total Environ 596–597:256–265. https://doi.org/10.1016/j.scitotenv.2017.04.080

LIBERTE-ALGERIE.COM (2019) Croissance démographiques: La population algérienne a connu un véritable «boom». algerie360.com 1

Lubowski RN, Vesterby M, Bucholtz S et al (2006) Major uses of land in the United States:2002

Ma Z, Redmond RL (1995) Tau coefficient for accuracy assessment of classification of remote sensing data. Photogrametric Eng Remote Sens Soc 61:435–439

Macleod RD, Congalton RG (1998) A quantitative comparison of change-detection algorithms for monitoring eelgrass from remotely sensed data. Photogramm Eng Remote Sens 64:207–216

McFeeters SK (1996) The use of the normalized difference water index (NDWI) in the delineation of open water features. Int J Remote Sens 17:1425–1432. https://doi.org/10.1080/01431169608948714

Michalowska K, Glowienka E, Hejmanowska B (2016) Temporal satellite images in the process of automatic efficient detection of changes of the Baltic Sea coastal zone. In: IOP conference series: earth and environmental science

Ministère de L'Agriculture DGDBEDGTH (2019) Situation Hydraulique des Barrages

Mlayah A, Ferreira da Silva E, Rocha F, Hamza CB, Charef A, Noronha F (2009) The Oued Mellègue: mining activity, stream sediments and dispersion of base metals in natural environments, North-Western Tunisia. J Geochem Explor 102:27–36. https://doi.org/10.1016/j.gexplo.2008.11.016

Mlayah A, Ferreira Da Silva EA, Lachaal F et al (2013) Effet autoépurateur de la lithologie des affleurements géologiques dans un climat semi-aride: cas du bassin versant de l'Oued Mellègue (Nord-Ouest de la Tunisie). Hydrol Sci J 58:686–705. https://doi.org/10.1080/02626667.2013.772300

Mlayah A, Lachaal F, Chekirbane A, Khadar S, da Silva EF (2017) The fate of base metals in the environment and water quality in the Mellegue Watershed, Northwest Tunisia. Mine Water Environ 36:163–179. https://doi.org/10.1007/s10230-017-0430-z

Niu X, Tang J, Wang S, Fu C (2018) Impact of future land use and land cover change on temperature projections over East Asia. Clim Dyn 52:6475–6490. https://doi.org/10.1007/s00382-018-4525-4

Paola JD, Schowengerdt RA (1995) A detailed comparison of backpropagation neural network and maximum-likelihood classifiers for urban land use classification. Geosci Remote Sensing, IEEE Trans 33:981–996. https://doi.org/10.1109/36.406684

Pauleit S, Ennos R, Golding Y (2005) Modeling the environmental impacts of urban land use and land cover change—a study in Merseyside, UK. Landsc Urban Plan 71:295–310. https://doi.org/10.1016/j.landurbplan.2004.03.009

Pielke RA, Adegoke J, Beltrán-Przekurat A et al (2007) An overview of regional land-use and land-cover impacts on rainfall. Tellus Ser B Chem Phys Meteorol 59:587–601. https://doi.org/10.1111/j.1600-0889.2007.00251.x

République Tunisienne - Ministère de l'Agriculture et des Ressources Hydrauliques et de la Pêche (2015) Filières légumes. République Tunisienne - Ministère l'Agriculture des Ressources Hydraul. la Pêche, In http://www.gil.com.tn/fr/staticPage?label=filieres-legumes_4

Rimal B (2011) Application of Remote Sensing and Gis , Land Use / Land Cover Change in Kathmandu Metropolitan City , Nepal . J Theor Appl Inf Technol

Sentian J, Kong SSK (2015) The effect of land cover changes on surface temperature and precipitation in the Southeast Asia region. Adv Sci Lett 21:181–184. https://doi.org/10.1166/asl.2015.5849

Singh A (1989) Review article: digital change detection techniques using remotely-sensed data. Int J Remote Sens 10:989–1003. https://doi.org/10.1080/01431168908903939

Singh P, Kikon N, Verma P (2017) Impact of land use change and urbanization on urban heat island in Lucknow city, Central India. A remote sensing based estimate. Sustain Cities Soc 32:100–114. https://doi.org/10.1016/j.scs.2017.02.018

Sundara Kumar K, Udaya Bhaskar P, Padmakumari K (2015) Application Of Land Change Modeler For Prediction Of Future Land Use Land Cover A Case Study Of Vijayawada City. In: International Conference on Science, Technology and Management. New Delhi(India), pp 2571–2581

Taylor CM (2002) The Influence of Land Use Change on Climate in the Sahel. J Clim 15:3615–3629. https://doi.org/10.1175/1520-0442(2002)015<3615:TIOLUC>2.0.CO;2

Telkar S (2017) Concept of watershed management and its components

Treitz P, Rogan J (2004) Remote sensing for mapping and monitoring land-cover and land-use change—an introduction. Prog Plan 61:269–279. https://doi.org/10.1016/s0305-9006(03)00064-3

Tunisian Republic, Ministry of industry (2016) Tunisian olive oil|packaged olive oil| organic olive oil. Tunisian olive oil. In: Tunis, olive oil http://www.tunisia-oliveoil.com/En/.

Université de Sherbrooke - Québec - Canada (2020) Perspective Monde, Croissance Annuelle de la Population, Algérie. Ec. Polit. Appliquée, Fac. dess Lettres Sci. Hum. Univ. Sherbrooke, Québec, Canada http://perspective.usherbrooke.ca/bilan/tend/DZA/fr/SP.POP.TOTL.html?fbclid=IwAR3yf5bJpYiyw1-oVDhebKlsnlRm3sbc1_atuQvYSqBhi1XbGj1ieZ4Irhw

UTICA-TUNISIE (2011) Stratégie de développement des exportations tunisiennes des Services « Conseils aux Entreprises »

Van De Griend AA, Owe M (1993) On the relationship between thermal emissivity and the normalized difference vegetation index for natural surfaces. Int J Remote Sens 14:1119–1131. https://doi.org/10.1080/01431169308904400

Wang P, Yamanaka T, Qiu GY (2012) Causes of decreased reference evapotranspiration and pan evaporation in the Jinghe River

catchment, northern China. Environmentalist 32:1–10. https://doi.org/10.1007/s10669-011-9359-0

Weng Q, Lu D, Schubring J (2004) Estimation of land surface temperature-vegetation abundance relationship for urban heat island studies. Remote Sens Environ 89:467–483. https://doi.org/10.1016/j.rse.2003.11.005

www.flehetna.com (2018) Algérie: Hausse de 70% de la superficie plantée en arbres fruitiers. http://www.flehetna.com/fr 1

Xie Y, Shi J, Lei Y, et al (2014) Impacts of land cover change on simulating precipitation in Beijing area of China State Key Laboratory of Remote Sensing Science, Institute of Remote Sensing and Digital Earth, Chinese Academy of Sciences, Beijing, 100101, China. University of Chine. 4145–4148

Yacouba D, Guangdao H, Xingping W (2009) Applications of remote sensing in land use/land cover change detection in Puer and Simao counties, Yunnan Province. J Am Sci 5:157–166

Yang X, Ren L, Singh VP, Liu X, Yuan F, Jiang S, Yong B (2012) Impacts of land use and land cover changes on evapotranspiration and runoff at Shalamulun River watershed, China. Hydrol Res 43: 23–37. https://doi.org/10.2166/nh.2011.120

Youneszadeh S, Amiri N, Pilesjo P (2015) The effect of land use change on land surface temperature in the netherlands. In: International Conference on Sensors & Models in Remote Sensing & Photogrammetry. The International Archives of the Photogrammetry, Remote Sensing and Spatial Information Sciences, Volume, pp 23–25

Zhang X, Liu L, Henebry GM (2019) Impacts of land cover and land use change on long-term trend of land surface phenology: a case study in agricultural ecosystems. Environ Res Lett 14. https://doi.org/10.1088/1748-9326/ab04d2